Figure 1: Snapshot ~~for~~ density $\rho = 0.95$ and $k_B T = 1.5$. ~~Arrows~~ represent the dipole moment of the particle. ~~Obtained by means of Langevin dynamics simulation.~~ The simulation was allowed to equilibrate for time $t = $ 100 ~~with fluid medium viscosity~~ ~~$\eta = 1$ and particle mass $m = 1$.~~

1 Model

We consider colloidal particles with a permanent dipole moment $\mu\hat{m}$, where $\hat{m}$ is a unitary vector with the direction of the dipole moment. While considering a three-dimensional system, we constrain particle translational motion to a one-dimensional line, i.e. particles are confined to the z axis. However, particles can explore the full three-dimensional orientation space. A snapshot of the system is shown in the Figure 1.

The particle-particle interaction is described as the superposition of two contributions: a dipole-dipole interaction and a short-range repulsion.

The energy of dipole-dipole interaction for any pair (i, j) of particles is given by

$$U_{ij}^{dip} = -\frac{\mu_i \mu_j}{\Delta r^3}[3(\hat{m}_i \cdot \hat{r}_{ij})(\hat{m}_j \cdot \hat{r}_{ij}) - (\hat{m}_i \cdot \hat{m}_j)] \tag{1}$$

where $\mu_i \hat{m}_i$ and $\mu_j \hat{m}_j$ are dipole moments of interacting particles, $\boldsymbol{r}_{ij}$ is the ~~direction~~ vector which connects particle centers, and Δr is the absolute value of the distance between particle centers.

By constraining particles to a 1D tube we effectively enforce $\boldsymbol{r}_{ij}$ to be co-aligned with z axis. Assuming that all particles have the same dipole moment $\mu_i = \mu_j = \mu$, and defining $\mu = 1$ (1) can be simplified as:

$$E_{ij}^{dip} = -\frac{1}{\Delta z^3}[3\cos\theta_i \cos\theta_j - (\hat{m}_i \cdot \hat{m}_j)] \tag{2}$$

where θ_i and θ_j are the angles between z axis and dipole moments of the first and second particle, respectively, and $\Delta z = |z_j - z_i|$, where z_i and z_j are particle positions along the z axis.

The repulsive part is described by Yukawa potential

$$E_{ij}^{rep} = \frac{A\exp(-k\Delta z)}{\Delta z}, \tag{3}$$

where A and k^{-1} are the strength and range of interaction.

In this work we define thermal energy ϵ as fraction of dipole-dipole interaction potential, i.e. $\epsilon = k_B T \mu^2$, and maintaining the ration between μ and A as constant. Since $\mu = 1$, we will use $k_B T$ to denote thermal energy. I mean, it's the same value, but different units, right

Figure 2 shows some examples of E_{ij} for different parameters.

When the dipole moments are perpendicular to each other, the interaction is purely repulsive for any given A and k.

However, as we can see on the Figs. 2(a) and (b), for co-aligned configurations for significantly low values of A and high values of k, the interaction is purely attractive. We will not consider those cases, as the system will be unstable and all particles will ~~coalesce in~~ one point. In this work, to reduce the number of free-parameters we fix $A = 1000\mu$ and $k = 10$. The k is inverse distance, right?
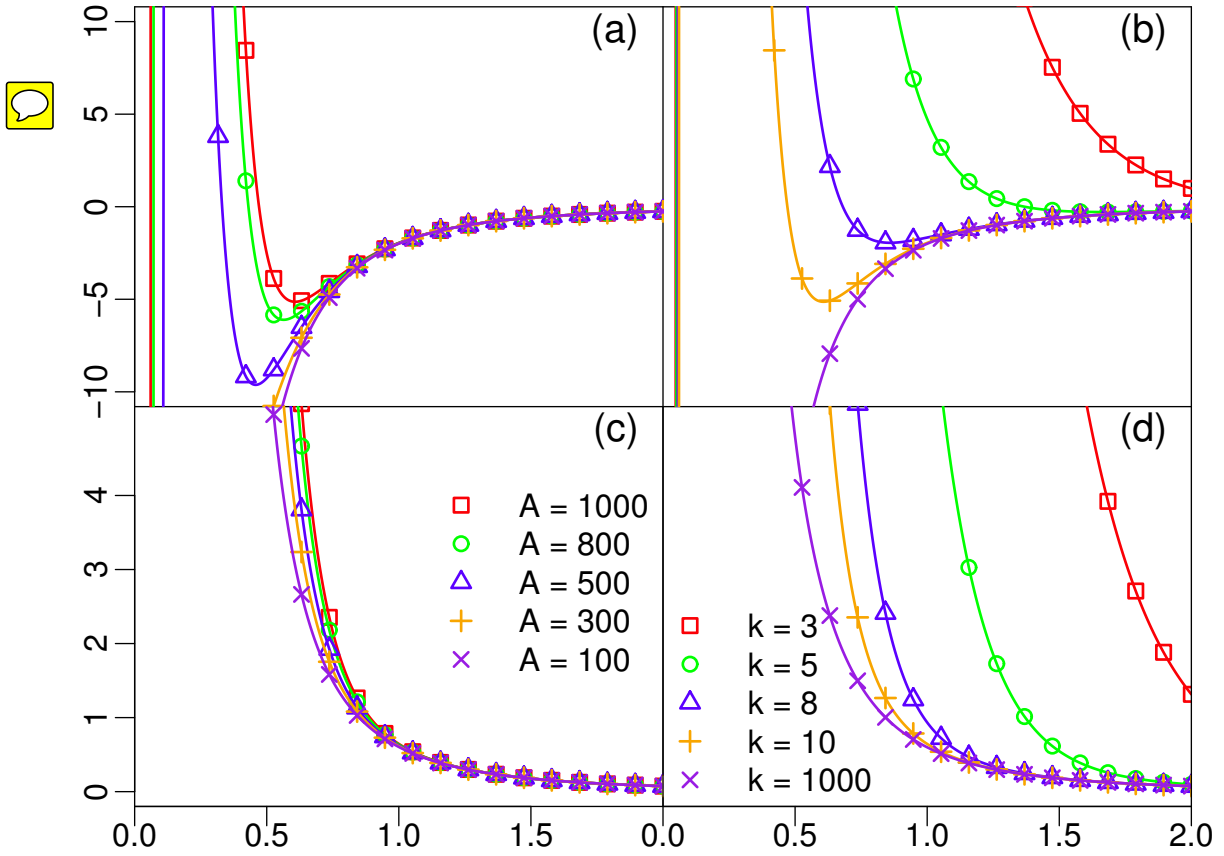
1

Figure 2: Potential energy as function of the interparticle distance when the dipoles are aligned (top) and perpendicular (bottom) ~~orientation of the particles dipole moments~~. Left plots the interparticle distance when the dipoles are for $k = 10$, and right the right ones for $A = 1000$.
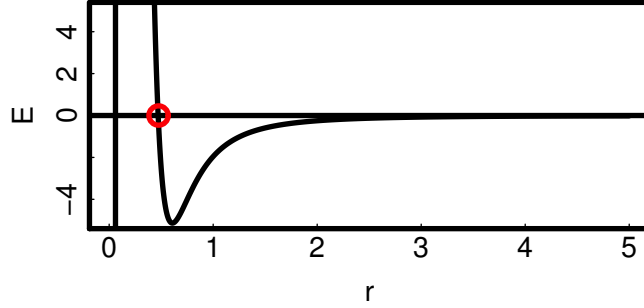
Figure 3: Potential energy as function of interparticle distance for co-aligned configuration and $k = 10$, $A = 1000$. Red point shows location of Δz_0

2   Monte Carlo Simulations

First, we study the equilibrium properties by means of Monte Carlo simulations.

At first Monte Carlo step we select a particle at random, and attempt a translational and then a rotational move. Next step we select the first neighboring particle in the positive direction of z axis. And repeat translational and rotational move

In the translational move a particle is displaced along the z-axis ($z_{t+1} = z_t + \delta z$), where δz is a random value uniformly distributed in the range $[+\eta, -\eta]$, with $\eta = 0.5(\Delta z_{min} - \Delta z_0)$. Here Δz_{min} is the interparticle distance for which the interaction energy between two aligned dipoles is minimal, and Δz_0 is the interparticle distance for which the potential energy vanishes if we decrease distance starting from Δz_{min}. Δz_0 is shown as red circle at the Fig. 3.

For the rotational move a new orientation is chosen uniformly at random. A move is accepted with probability $\eta < \min\{1, \exp(\Delta E/k_B T)\}$, where η is a random number uniformly-distributed in $[0, 1)$ and ΔE is change in potential energy due to the trial move.

For the sake of simplicity, we restrict interactions to the first-neighbors.

We also consider periodic boundary conditions.

3   Simulation details

Defining $\rho = \frac{ND}{L}$ where N — number of particles and $D = \Delta z_{min}$ — particle diameter calculated numerically, we immediately obtain the simulation system size $L = ND/\rho$. In our simulations we considered cases of different densities $\rho = (0.25,\ 0.5,\ 0.75)$.

To check for existence of finite-size effects, for each value of density we performed simulations with different system sizes $N = (1600,\ 3200,\ 6400)$. I'm maintaining density as constant and changing L and N accordingly. I'm reporting here N instead of L because the particle diameter is 0.62, and for $N = 1600, \rho = 0.75$ the $L = 1322.667$, which for me is more confusing then number of particles

The Monte-Carlo simulations were allowed to equilibrate for $\Delta = 3 \cdot 10^5$ Monte Carlo sweeps, and different quantities were measured after every Δ sweeps, obtaining 10 uncorrelated samples. To generate the initial configuration, dipolar particles were regularly distributed along z axis, with an interparticle distance $d = \frac{D}{\rho}$, and then displaced by a certain value, following a uniform distribution in the range $[-d/4, d/4]$. The orientation of the dipoles was generated uniformly

random.

The Langevin dynamics simulations were ran with the following parameters: unitary mass m and viscosity μ, and time integration step $dt = 0.01$. Initial particle coordinates were obtained as in the Monte-Carlo case. To check dependence of system evolution on the initial configuration, we performed simulations staring from three possible orientational configurations. First, we generated the initial orientations uniformly at random; second, we aligned all particles along the z axis; and third, particles of even index were oriented along, and with odd index against z axis. We refer to these configurations as "random", "co-aligned" and "counter-aligned", respectively. The sampling was done directly — ensemble averaging quantities over one simulation run, we obtain one uncorrelated sample.

We measured the following quantities:

Nematic order parameter S is defined as:

$$S = \frac{3\langle \cos^2 \theta \rangle - 1}{2}, \tag{4}$$

where θ it the angle between particle dipole moment and z axis, while angle brackets denotes ensemble average over all particles.

Next we measured probability distribution $p(\theta)$ of the angle θ between particle dipole moment and z axis.

We also measured the orientation correlation as a function of the distance between particles:

$$C(\Delta z) = \langle \cos \theta_i \cos \theta_j \rangle, \tag{5}$$

where θ_i and θ_j are angles between spatial axis and dipole moments of particles for which $\Delta z - \delta < |z_j - z_i| \leq \Delta z + \delta$, where 2δ is a predefined space sampling. Angle brackets denotes ensemble-averaging over all particles in all samples which satisfy distance criteria.

We measure the average chain length, where chain is a sequence of chained particles and two particles considered to be "chained" if

$$\begin{cases} |z_i - z_j| \leq d \\ \theta_{i,j} \leq \alpha \text{ or } \theta_{i,j} \geq \pi - \alpha \end{cases} \tag{6}$$

where d is a predefined separation distance after which particles are "unchained", and second condition makes particles to be oriented in the same direction and within a certain angle α along or against z axis positive direction.

Using the same definition for a chain, we define one to be "right" chain if all the particles satisfy $\theta_i \leq \alpha$, "left" if $\theta_i \geq \pi - \alpha$, and "undefined" in all other cases. Then we can measure the probability of two neighbouring chains to be "left-left" or "left-right", etc.

For Langevin Dynamics we additionally measure autocorrelation function of a particle orientation:

$$C(t) = \langle \cos \theta_i(t) \cdot \cos \theta_i(0) \rangle \tag{7}$$

here $\theta_i(0)$ is the orientation of a particle i at the beginning of simulation and $\theta_i(t)$ is the orientation of the same particle in the same sample at the time t. The ensemble-averaging is done over all particles.

3.1 Equilibrium results

First, we study the relation between the order parameter (4) and $k_B T$ at equilibrium for different system densities. As we can see on the Figure 4, the nematic order increases with decrease of $k_B T$. The results are average over 200 samples. Important to observer rapid increase in order

parameter with the decay of thermal energy. The region of rapid increase shifts with densities, and for higher density the relation between order parameter and k_BT closer to linear. As we can see, there is no systematic scaling with system size. In the section 4 we will discuss LD system relaxation towards the equilibrium results. ~~Additionally important to note that the order parameter versus thermal energy dependency does not exhibit any criticality.~~ The results are consistent with reported in literature (see [3]). We must also note that statistical errors observed are of order 10^{-3}.
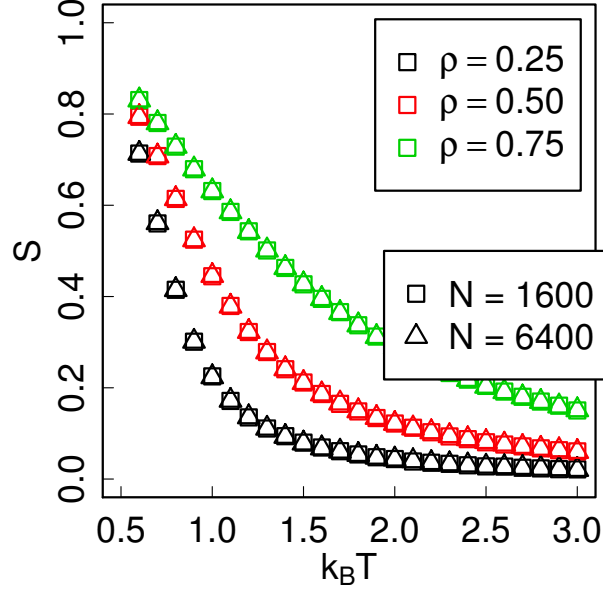

Figure 4: Order parameter defined by Eq. (4) versus k_BT for Monte-Carlo simulations. Triangles shows results for $N = 6400$ and squares for $N = 1600$ particles. As we can see there is no systematic scaling with system size. The results are obtained by means of MC simulations, and are average over 200 samples as described in sec. ??

To characterize the dependence of the structure on k_BT, we analyze the orientation correlation (i.e. the level of co-alignment) of particles as function of distance between them. For all ~~observed~~ range of simulation parameters the correlation (~~i.e. co-alignment between dipole moments of two particles~~) decays exponentially with distance. For selected number of simulation parameters the results are presented ~~at the~~ Figure 5, done in log-linear scale. The dots are obtained with space sampling $\delta = 1/6$, and are averaged over 200 samples with $N = 6400$ particles. Lines are obtained by linear approximation of the results in range $0.01 < C(\Delta z) < 0.45$.

The exponential decay of correlation with length for every combination of simulation parameters shows that we do not have any critical transition occurring in the system under study, despite non-zero order parameter observed above.

We could now write $C(\Delta z)$ as

$$C(\Delta z) \propto \exp\left[-\frac{\Delta z}{r^*(k_BT, \rho)}\right] \tag{8}$$

where r^* is the correlation length and depends on the system density and k_BT. The dependence of r^* on the k_BT for different system densities is shown at the Figure 6. We must note the similarity in behaviour of order parameter and the correlation distance. Additionally, the correlation distance never ~~approaches the infinity~~ for non-zero k_BT. ~~The relation is likely power law, do I need to mention this and add picture?~~

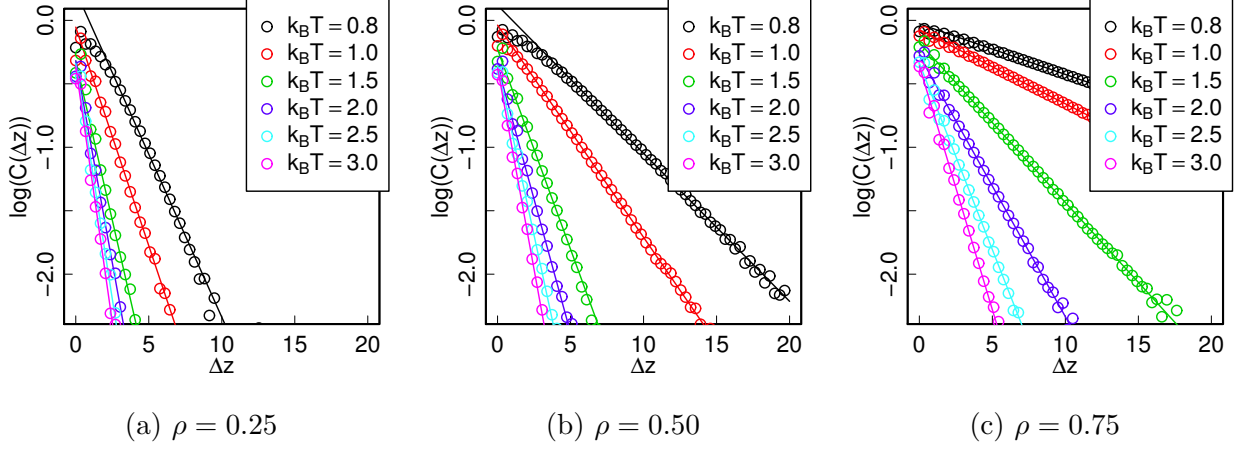|		
(a) $\rho = 0.25$	(b) $\rho = 0.50$	(c) $\rho = 0.75$

Figure 5: Orientation correlation as function of distance defined by Eq. (5) for Monte-Carlo simulations in the log-linear scale. The points are calculated for simulations with $N = 6400$ particles and the results are averaged over 200 samples as described in sec. **??**. Lines are obtained by linear approximation of the results in range $0.01 < C(\Delta z) < 0.45$.

4 Langevin Dynamics

4.1 Langevin equations

To study dynamics we ran Langevin dynamics simulations. Accordingly, each particle trajectory is obtained by solving two stochastic differential equations,

$$\dot{\boldsymbol{r}}(t) = \boldsymbol{v}(t) \tag{9}$$

and

$$m\dot{\boldsymbol{v}}(t) = \boldsymbol{f}(\boldsymbol{r}, t) - \alpha_{tr}\boldsymbol{v}(t) + \boldsymbol{\beta}_{tr}(t), \tag{10}$$

where m is the particle mass, $\boldsymbol{r}$ and $\boldsymbol{v}$ are the particle coordinates and velocity, α_{tr} is the damping coefficient related to the drag I think it's rather relevant that its drag from surrounding medium and not other particles, or its just obvious?, and $f(r, t)$ is a force acting on a particle, which comprises of interparticular interaction and external forces like some external potential, which we currently do not have. $\boldsymbol{\beta}_{tr}$ is a stochastic force, and in order to satisfy dissipation-fluctuation theorem, every component of it is assumed to be Gaussian-distributed, with

$$\langle \beta_{tr}(t) \rangle = 0 \tag{11}$$

and

$$\langle \beta_{tr}(t)\beta_{tr}(t') \rangle = 2\alpha_{tr}k_B T\delta(t - t'), \tag{12}$$

where k_B is the Boltzmann constant, T is thermostat temperature, δ is the Dirac delta function and the average is an ensemble average.

The trajectory of rotation motion is obtained by solving two stochastic differential equations,

$$\dot{\boldsymbol{\phi}}(t) = \boldsymbol{\omega}(t) \tag{13}$$

and

$$m\dot{\boldsymbol{\omega}}(t) = \boldsymbol{\tau}(r, t) - \alpha_r\boldsymbol{\omega}(t) + \boldsymbol{\beta}_r(t), \tag{14}$$

where ϕ is particle orientation angles, ω is the angular velocity, I is the inertia and τ is the torque exerted on a particle By other particles or external field alike. $\boldsymbol{\beta}_r(t)$ is the torque
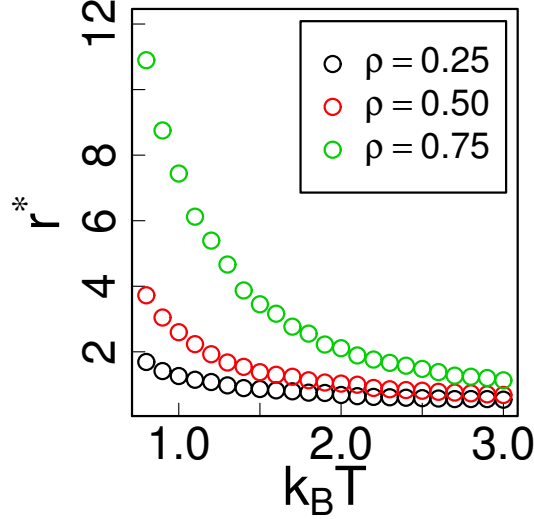
Figure 6: r^* as defined in (8), obtained as inverse slope of orientation correlation shown at Figure 5.

resulting from stochastic force rotating particle, and its components are also assumed to be Gaussian-distributed with zero mean

As we can see from Eqs. (9, 10, 13, 14), for the rotational motion the form of equations remains unchanged, and they are equivalent to the translation equations under following transformation.

$$
\begin{aligned}
\boldsymbol{\phi} &\to \boldsymbol{r} & I &\to m \\
\boldsymbol{\omega} &\to \boldsymbol{v} & \boldsymbol{\tau}(r,t) &\to \boldsymbol{f}(r,t)
\end{aligned}
\tag{15}
$$

The scalar values are transformed as is, while vectors are replaced with pseudo-vectors.

The damping coefficients α for translation (α_{tr}) and rotation (α_r) are different, and can be obtained in following way.

First to simplify the particle-medium interaction we need to define damping time τ, which determines how rapidly thermal fluctuations in particles positions and orientations decays, and for translational motion it is given by

$$
\tau_{tr} = \frac{m}{6\pi\eta R},
\tag{16}
$$

where m is the particle mass, η is the viscosity and R is the particle radius. For rotation $\tau_{tr}/\tau_r = 10/3$, which can be obtained from Stokes-Einstein-Debye relations and relation between particle mass and inertia.

And then the α_t and α_r are defined

$$
\alpha_{tr} = \frac{m}{\tau_{tr}} \qquad \alpha_r = \frac{I}{\tau_r},
\tag{17}
$$

where m is the particle mass, I is the inertia, $\tau_{tr,r}$ are the damping times.

4.2 Integration method

The integration scheme for translational equations of motion proposed in [2] is as follows

$$
\boldsymbol{r}^{n+1} = \boldsymbol{r}^n + dt \left(b_{tr}\boldsymbol{v}^n + \frac{b_{tr}dt}{2m}\boldsymbol{f}^n + \frac{b_{tr}}{2m}\boldsymbol{\beta}_{tr}^{n+1} \right)
\tag{18}
$$

$$\boldsymbol{v}^{n+1} = \boldsymbol{v}^n + \frac{dt}{2m}\left(\boldsymbol{f}^n + \boldsymbol{f}^{n+1}\right) - \frac{\alpha_t}{m}\left(\boldsymbol{r}^{n+1} - \boldsymbol{r}^n\right) + \frac{1}{m}\boldsymbol{\beta}_{tr}^{n+1}. \tag{19}$$

In the above equations, the dt is integration time step, the n index is time steps, b_{tr} accounts for the drag, and $\boldsymbol{\beta}_{tr}^{n+1}$ is a stochastic force at the time $n+1$. Important to note that we use the same stochastic force for coordinates and velocity calculations, which reduces computation time. $\boldsymbol{f}^n$ is the force acting on the particle at the time n. the $_{tr}$ index is for the translation, it's now consistent with what was above. Do I need to specifically state it? The index $^{n+1}$ in the random term due to that at $n = 0$ there is no random force. Anyway, as long as it's only one random force it's all the same - they are all uncorrelated

The same integration scheme can be used for rotation, with proper change of variables (see Eq. (15))

$$\boldsymbol{\phi}^{n+1} = \boldsymbol{\phi}^n + dt\left(b_r\boldsymbol{\omega}^n + \frac{b_r dt}{2I}\boldsymbol{\tau}^n + \frac{b_r}{2I}\boldsymbol{\beta}_r^{n+1}\right) \tag{20}$$

$$\boldsymbol{\omega}^{n+1} = \boldsymbol{\omega}^n + \frac{dt}{2m}\left(\boldsymbol{\tau}^n + \boldsymbol{\tau}^{n+1}\right) - \frac{\alpha_r}{I}\Delta\boldsymbol{u} + \frac{1}{I}\boldsymbol{\beta}_r^{n+1} \tag{21}$$

here $\Delta\boldsymbol{u} \equiv \left(\boldsymbol{\phi}^{n+1} - \boldsymbol{\phi}^n\right)$ is rotation of the particle within one integration step. Vector Δu is parallel to the axis around which particle has rotated on the angle $|\Delta u|$ radians. The coefficients b_{tr} and b_r account for the drag exerted on a particle by surrounding medium,

$$b_{tr} = \frac{1}{1 + \frac{\alpha_{tr} dt}{2m}} \qquad \text{and} \qquad b_r = \frac{1}{1 + \frac{\alpha_r dt}{2I}}. \tag{22}$$

I think I'm doing it wrong, but that period mark after the equation is really confusing

When $\alpha_{tr} = 0$, from Eq. (22), we obtain $b_{tr} = 1$ and from Eq. (12) we obtain $\langle\beta_{tr}(t)\beta_{tr}(t')\rangle = 0$. Then the above equations reduces to the standard velocity-Verlet scheme. The damping is calculated as integral over real path travelled by particle within time step (under assumption that damping time does not change within dt and Δr) Yes, the damping time is constant, but if it isn't, this assumption is enough for this scheme to work. I never said that it isn't a constant.

If using integration scheme defined in Eq. (20), effective angular velocity of a particle within every time step is

$$\tilde{\boldsymbol{\omega}}^n = b_r\boldsymbol{\omega}^n + \frac{b_r dt}{2I}\boldsymbol{\tau}^n + \frac{b_r}{2I}\boldsymbol{\beta}_r^{n+1}. \tag{23}$$

By the definition, angular velocity $\tilde{\boldsymbol{\omega}}^n$ is directed parallel to the axis around which particle is rotated by an angle of $|\tilde{\boldsymbol{\omega}}^n|dt$ per time step dt. Therefore, if particle orientation is defined by quaternion q, then Eq. (20) can be written as

$$q^{n+1} = \tilde{q}^n q^n, \tag{24}$$

where q^n and q^{n+1} is the quaternion representation of orientation on time steps n and $n+1$ respectively, and $\tilde{q}^n q^n$ is quaternion multiplication. $\tilde{q}^n$ is the quaternion representation of rotation around $\tilde{\boldsymbol{\omega}}^n$ by the angle $|\tilde{\boldsymbol{\omega}}^n|$.

4.3 Interactions

To perform simulations we need to define forces acting on the particles.

First of all, as in the Monte-Carlo simulations we restrict interactions to the immediate neighbors (particle i interacts only with particles $i+1$ and $i-1$).

The force acting on a particle is defined by gradient of potential energy.

$$\boldsymbol{F}_{ij} = -\boldsymbol{\nabla}E_{ij} = \frac{\hat{r}}{r^4}\left[3D - A\,r^2(kr+1)\exp(-kr)\right], \tag{25}$$

where $D = 3\cos\theta_1\cos\theta_2 - (\hat{m}_1 \cdot \hat{m}_2)$ stands for orientational part of dipole-dipole potential and r connects particle centers. The other parameters are the same as in Eqs. (2) and (3).

The torque on a particle results only from the dipole-dipole interaction. Therefore it is calculated as

$$\boldsymbol{\tau} = \mu[\hat{\mu} \times \boldsymbol{E}_d], \tag{26}$$

where $\boldsymbol{\mu}$ is dipole moment of particle on which torque acts, and $\boldsymbol{E}_d$ is dipole field produced by acting particle:

$$\boldsymbol{E}_d = \frac{\mu}{r^3}\left(3(\hat{\mu} \cdot \hat{r})\hat{r} - \hat{\mu}\right), \tag{27}$$

where μ is dipole moment of the particle inducing the field.

4.4   Statistical properties

For non-interacting spheres the relation between rotational and translational diffusion coefficient can be obtained [1]. The former is given by the Stokes-Einstein relation

$$D_t = \frac{k_B T}{6\pi\eta R} \tag{28}$$

and the latter is given by Stokes-Einstein-Debye relation

$$D_r = \frac{k_B T}{8\pi\eta R^3}, \tag{29}$$

where T is the thermostat temperature, η the viscosity of the medium and k_B the Boltzmann constant. The relation between D_t and D_r is given by

$$\frac{D_r}{D_t} = \frac{3}{4R^2}. \tag{30}$$

For sufficiently long times, we can estimate the diffusion coefficient as

$$D_t = \lim_{\Delta t \to \infty} \frac{1}{6\Delta t}\langle r^2(\Delta t)\rangle, \tag{31}$$

where $\langle r^2(\Delta t)\rangle$ is translational mean square displacement (MSD) of particle relatively to its initial position,

$$\langle r^2(\Delta t)\rangle = \frac{1}{N}\sum_{i=1}^{N}|\boldsymbol{r}_i(t+\Delta t) - \boldsymbol{r}_i(t)|^2. \tag{32}$$

Analogously can be defined relation between rotational diffusion coefficient D_r and rotational mean square displacement (RMSD) $\langle\phi^2(\Delta t)\rangle$

$$D_r = \lim_{\Delta t \to \infty} \frac{1}{6\Delta t}\langle\phi^2(\Delta t)\rangle. \tag{33}$$

The vector Δu of rotational displacement between two particle orientations represented by quaternions q^{n+1} and q^n can be found in the following way. First, we obtain quaternion $\Delta q = q^{n+1}q^{n^{-1}}$, where $q^{n^{-1}}$ is the inverse of q^n. Then the direction of Δu is parallel to the vector part of Δq and $|\Delta u|$ equals to the $\cos^{-1}$ of scalar part of Δq.

When calculating RMSD we have to account for the fact that rotations on angle α and $\alpha + 2\pi$ are represented by the same unit quaternions. For that we have to accumulate RD over integration steps (separately for every particle). Then the RMSD can be obtained:

$$\langle \phi^2(\Delta t) \rangle = \frac{1}{N} \sum_{i=1}^{N} \left| \sum_{j=0}^{\frac{\Delta t}{\delta t}} \Delta \boldsymbol{u}_{i,j} \right|^2 , \tag{34}$$

here we break time interval Δt into smaller time intervals δt, which is necessary due to inability to distinguish rotations on angle α and $\alpha + 2\pi$ radians. The accumulation of rotation goes under summation by j index. The Δt could be arbitrary big, so I need to sum the rotation over small intervals where particle turns less then 2π, or calculate the number of 2π rotations. The former is simpler to implement. It's like integrating over path, but splitted into small $\Delta t/\delta t$ pieces, on every one of which we can just use Δu

The results of test simulation of non-interacting spheres is shown on Figure 7. As expected, $\langle r^2 \rangle$ is proportional to $2 \cdot \tau_t t$, and $\langle \phi_i^2 \rangle$ are proportional to $2 \cdot \tau_r t = 2 \cdot (3/10)\tau_t t$. Here τ_t is translational damping time defined in eq. (16), and t is simulation time.
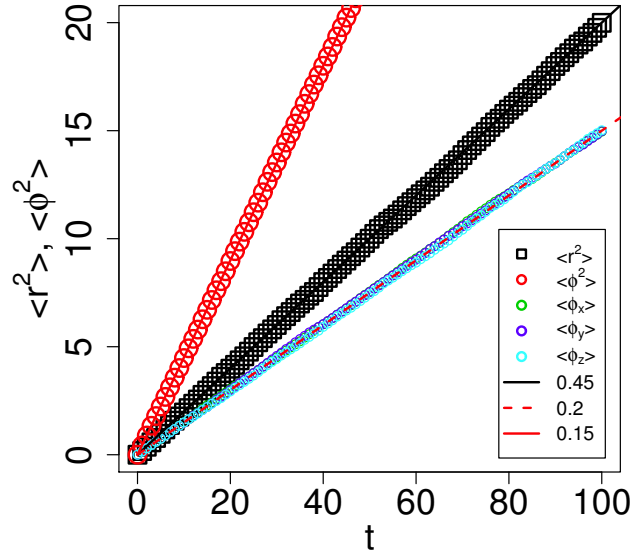

Figure 7: Particle MSD and RMSD (with components) as function of time. Points are obtained numerically, with averaging over 20000 samples. Every sample started from $r_z = v_z = \omega_i = 0$ and particle's dipole moment co-aligned with z axis. Solid lines are theoretical displacement (eqs. (31), (33)) for given $k_B T = 1$, $m = 1$, $R = 1$ and $\tau_t = 0.1$.

Average kinetic energy per degree of freedom is $1/2\,k_B T$, which for our case of full three-dimensional rotational and one-dimensional translational movement gives $E_k = 2k_B T$.

At equilibrium, velocity should satisfy Maxwell-Boltzmann distribution

$$p(v^2) = \sqrt{\left(\frac{m}{2\pi k_B T}\right)^3} 4\pi v^2 \exp\left[-\frac{mv_i^2}{2k_B T}\right] \qquad p(\omega^2) = \sqrt{\left(\frac{I}{2\pi k_B T}\right)^3} 4\pi \omega^2 \exp\left[-\frac{I\omega_i^2}{2k_B T}\right] \tag{35}$$

where v is translational and ω is rotational velocity, m is particle mass, and I is particle inertia, k_B is Boltzmann constant and T is thermodynamic temperature.

Velocity components should satisfy normal distribution

$$p(v_i) = \sqrt{\frac{m}{2\pi k_B T}} \exp\left[-\frac{mv_i^2}{2k_B T}\right] \qquad p(\omega_i) = \sqrt{\frac{I}{2\pi k_B T}} \exp\left[-\frac{I\omega_i^2}{2k_B T}\right] \tag{36}$$

It can be shown that ratio between $\sigma_v^2 = k_B T/m$ and $\sigma_\omega^2 = k_B T/I$ is

$$\frac{\sigma_v^2}{\sigma_\omega^2} = \frac{2}{3}R^2 \qquad (37)$$

where R is radius of a particle.

At the Figure 8 the velocity probability distribution are shown, both theoretical and obtained from simulations, for one value of $k_B T = 1$ and $m = 1$. As expected, the $\sigma_v^2/\sigma_\omega^2$ are related as $2/3$ for our case of $R = 1$.
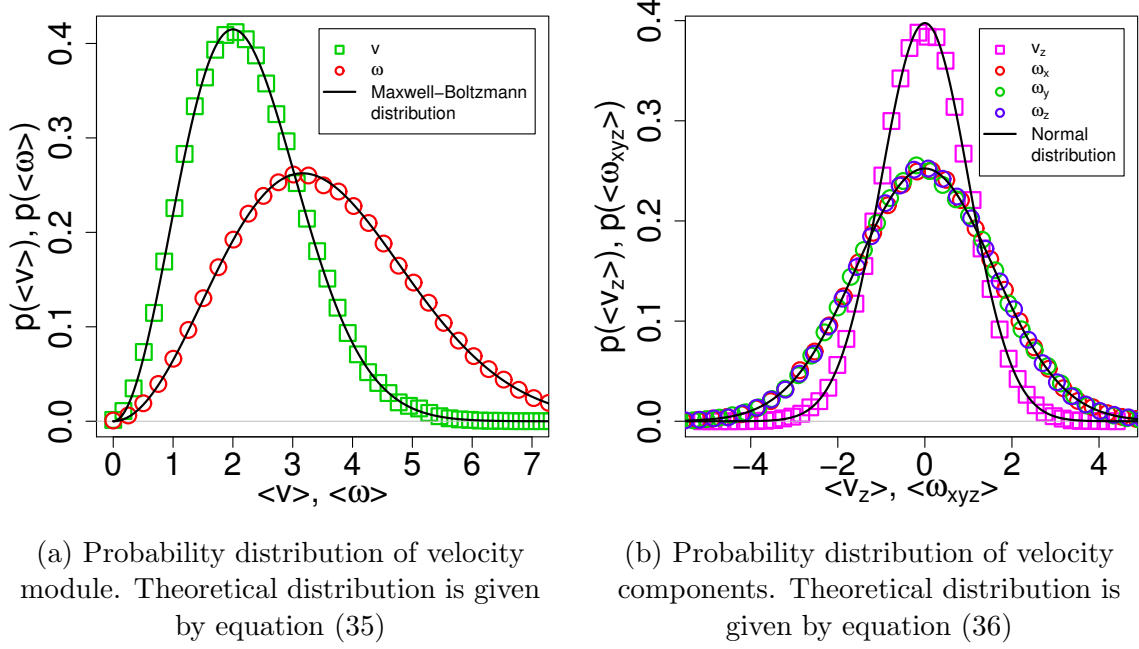

(a) Probability distribution of velocity module. Theoretical distribution is given by equation (35)

(b) Probability distribution of velocity components. Theoretical distribution is given by equation (36)

Figure 8: Translational and rotational velocity probability distribution. Points are obtained numerically, with averaging over 20000 samples. Every sample started from $r_z = v_z = \omega_i = 0$ and particle's dipole moment co-aligned with z axis. Solid lines are theoretical distributions for given $k_B T = 1$ and $m = 1$.

4.5 Dynamics results

To study the time evolution, we perform Langevin Dynamics simulation for a set of simulation parameters as described in Section 3.

The relaxation of the order parameter S defined in (4) to the equilibrium value ($|S - S_{eq}|$) is shown on the Fig. 9.

First thing to note is that notwithstanding the initial configuration, after initial rearrangement due to Effect, the relaxation shows the same behavior for low and moderate density for any given $k_B T$. The random configuration is closer to equilibrium, in the sense that there are particles pointing in both directions, so I'd say that it's, like, main relaxation line, and all other initial configurations will tend to get there.

The results suggest power law behavior in cases of low density $\rho = 0.75$, as we can see at the left side of Fig. 9.

For the high density, the relaxation occurs faster ~~then~~ for the low density. Because of this the statistical errors from Monte Carlo play greater role. To mitigate that, we simulate 1000 samples for the long time ($t_{max} = 1000$). Using this data, we presume that system is stable after $t_{EQ} = 800$, and after performing average over samples, we time-average results after that moment. While the results The long-time average and MC are within the statistical error

11

As we can see on the right side of Fig. 9, there are distinguishable high and low k_BT regimes. At the high $k_BT \geq 1.5$ the relaxation occurs fast and with high fluctuations, so it's hard to say anything. And there is little influence from the initial configuration. However, the low $k_BT \leq 1$ regime suggests exponential relaxation to the equilibrium results, and also it shows strong influence of initial configuration on the path and time of the relaxation.
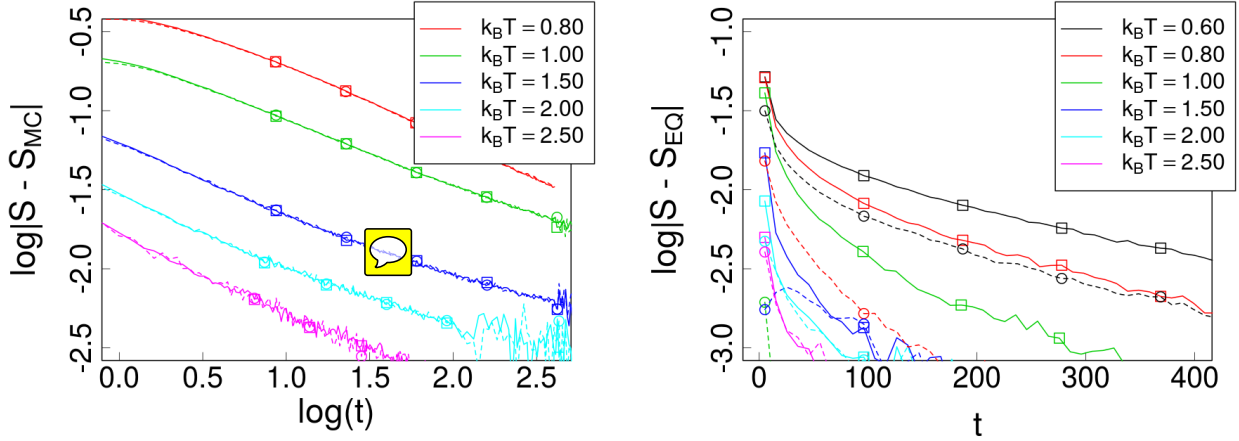

Figure 9: Relaxation of order parameter to the equilibrium values for densities $\rho = 0.25, 0.75$ in the left and right respectively. The squares denote co-aligned initial configuration, and circles stand for randomly-oriented configuration. The results are obtained on 500 samples.

To gain more insight on how the system evolves, we look into particle orientations relative to its neighbors. The main results are shown at the Fig. 10.

First of all, we need to note that due to the symmetry of the interaction potential, the equilibrium (i.e. Monte-Carlo) results for the pairs "LL" – "RR" and "LR" – "RL" are the same, accounting for the statistical error.

As above, the high and low densities show different behavior. Similar to order parameter, for the low density the relaxation for any of the given orientation pairs suggests power law behavior. Also is important that there is little difference in slope of co-aligned and counter-aligned orientation pairs, as well as little influence of the k_BT. add the slope values. The respective pairs ("LL" – "RR" and "LR" – "RL") quickly come to the same value? and then relaxes absolutely the same way.

For the high density the behavior is more complicated. First of all, the results suggest the exponential relaxation for prevalent (i.e. "RR") orientation pair, with the power strongly dependent on the k_BT. On the other hand, the minority orientation pair (i.e. "LL") relaxes differently after the initial moments. the closer to the EQ values, the bigger the difference. It's more like power law, but unclear.

Another observation is that co-aligned orientation pairs relaxes slower then counter-aligned. It can be attributed to their less favorable energy configuration, and therefore much lesser representation on the equilibrium.

The average autocorrelation of the particles orientation as the function of time is shown at the Fig. 11. The results clearly shows the exponential tail for any given k_BT and density. However for short time scale the behaviour isn't exponential. The exponential tail gives us the following relation: $C(t) \sim \exp[t/t^*]$, where t^* is the autocorrelation time. If we look how it
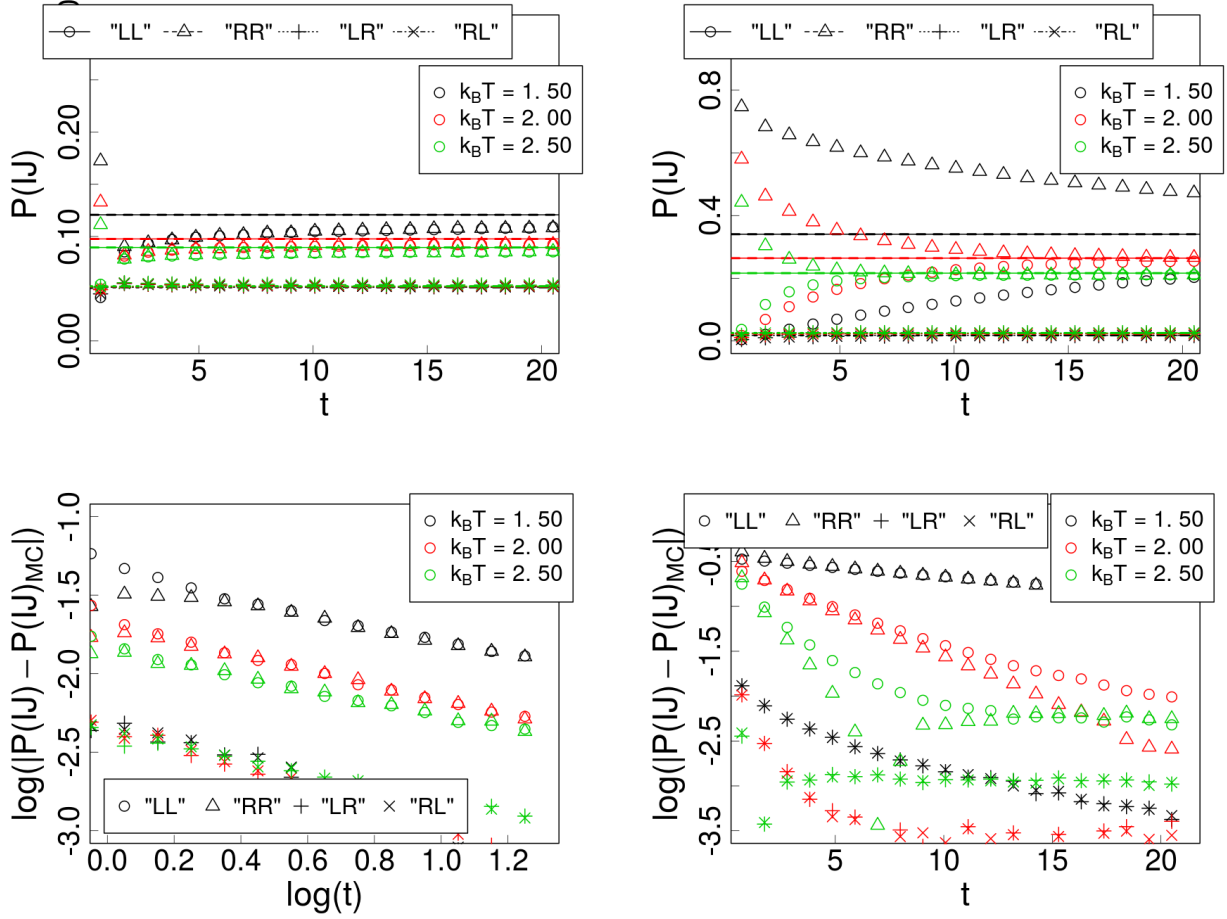
12

Figure 10: Relative particle orientation probabilities (top) and their relaxation to the equilibrium values (bottom), for low ($\rho = 0.25$) and high ($\rho = 0.75$) density at the left and right respectively. Lines show the equilibrium results, however, the pairs "LL" – "RR" and "LR" – "RL" values are indistinguishable at this scale. The simulations start from co-aligned initial configuration.

depends on density and k_BT, we obtain the results shown at the Fig. 12. We want to note here that the correlation time is longer for the co-aligned then it is for the random initial configuration, however, with increase in density the ratio between the two decreases. Need to check the 0.5 results, probably naming error.

5 Appendix

5.1 Quaternions

Quaternion $q = (\omega, \vec{a})$ with a norm $\|q\| = 1$ defines rotation around axis parallel to $\vec{a}$ on the angle $\cos^{-1}(2\omega)$.

One can define quaternion norm

$$\|q\| = |\omega| + \|\vec{a}\| \tag{38}$$

Quaternion conjugation

$$q^{-1} = (\omega, -\vec{a}) \tag{39}$$

And quaternion product

$$q_3 = q_1 q_2 = (\omega_1 \omega_2 - \vec{a}_1 \cdot \vec{a}_2, \quad \omega_1 \vec{a}_2 + \omega_2 \vec{a}_1 + [\vec{a}_1 \times \vec{a}_2]) \tag{40}$$

If we have a unit vector $\vec{a}_1$ and want to rotate the vector $\vec{r}$ around it on the angle ω_1, first we need to construct quaternion

$$q_1 = \left(\cos \left(\frac{\omega_1}{2} \right), \vec{a}_1 \sin \left(\frac{\omega_1}{2} \right) \right) \tag{41}$$

which represents the rotation $\mathbb{R}_1$, and then to apply $\mathbb{R}_1$ to $\vec{r}$

$$\vec{r}' = q_1 \vec{r} q_1^{-1} \tag{42}$$

where $\vec{r}'$ is the new state of the vector $\vec{r}$ after rotation, and q_1^{-1} is the quaternion conjugate to q_1.

Multiplication $q_i \vec{r}$ should be done by the rules of quaternion product (40). The vector $\vec{r}$ should be treated as quaternion $q_r = (0, \vec{r})$.

If we have a rotation $\mathbb{R}_1$ represented by quaternion q_1 and rotation $\mathbb{R}_2$ represented by quaternion q_2, and we want to apply them to vector $\vec{r}$ in order $\mathbb{R}_1$, $\mathbb{R}_2$, by definition (42) we can write

$$\vec{r}'' = q_2 \vec{r}' q_2^{-1} = q_2 q_1 \vec{r} q_1^{-1} q_2^{-1} \tag{43}$$

and if we define $q_3 = q_2 q_1$, then $q_3^{-1} = q_1^{-1} q_2^{-1}$ and then

$$\vec{r}'' = q_3 \vec{r} q_3^{-1} \tag{44}$$

Therefore, compound rotation of two sequential rotations which are represented by quaternions q_1 and q_2 is represented by quaternion $q_3 = q_2 q_1$, where $q_2 q_1$ is quaternion product (40). Rotation represented by the rightmost quaternion is applied first, then the one represented by the second-rightmost, and so on.

If we define a global reference frame, then any quaternion q can also define a rotated reference frame. To get coordinates $\vec{r}'$ of a vector $\vec{r}$ defined in global frame in rotated, one only have to apply quaternion q to vector $\vec{r}$. To go back to global reference frame from $\vec{r}'$, one have to apply q^{-1} to $\vec{r}'$.

$$\vec{r}' = q\vec{r}q^{-1} \qquad \vec{r} = q^{-1}\vec{r}'q \tag{45}$$

References

[1] C. S. Dias, C. Braga, N. A. M. Araujo, and M. M. da Gama. Relaxation dynamics of functionalized colloids on attractive substrates. *Soft Matter*, 2016.

[2] Niels Grønbech-Jensen and Oded Farago. A simple and effective Verlet-type algorithm for simulating Langevin dynamics. *Molecular Physics*, 111(8):983–991, apr 2013.

[3] Bennett D Marshall. Thermodynamic perturbation theory for associating fluids confined in a one-dimensional pore. *The Journal of chemical physics*, 142(23):234906, 2015.

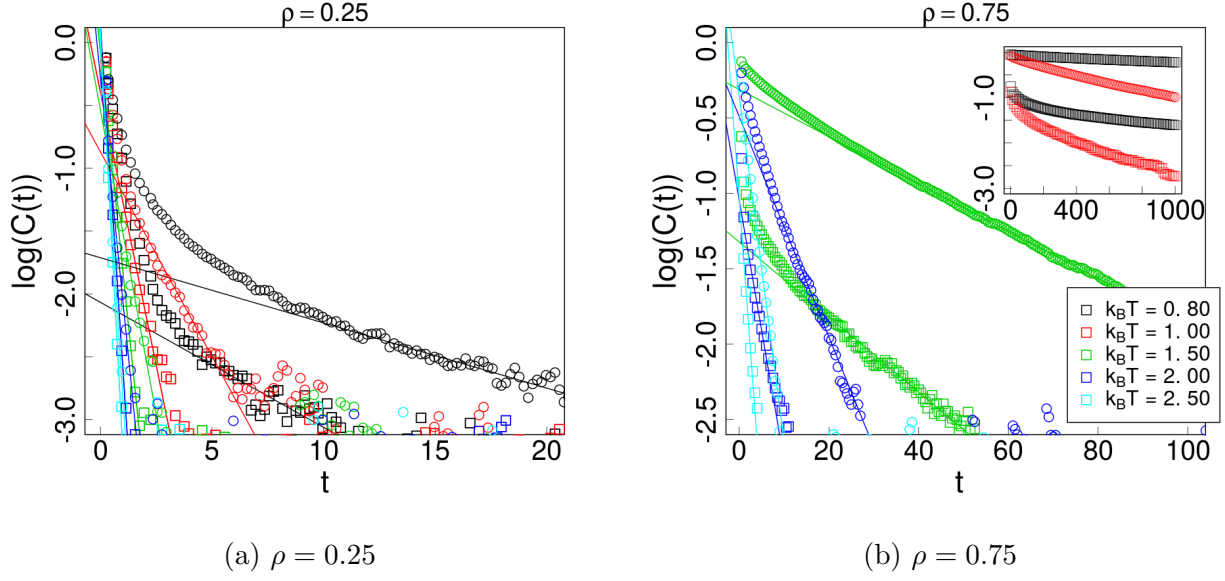(a) $\rho = 0.25$ (b) $\rho = 0.75$

Figure 11: Autocorrelation of particles orientation as function of time for LD simulations. The points are obtained as described in sec. 3. The squares correspond to random, and the circles corresponds to co-aligned initial configuration. Lines are the linear approximation to the data. I selected regions by hand, which looks the most linear, how can I say that?. Inset shows the results over bigger time frame.
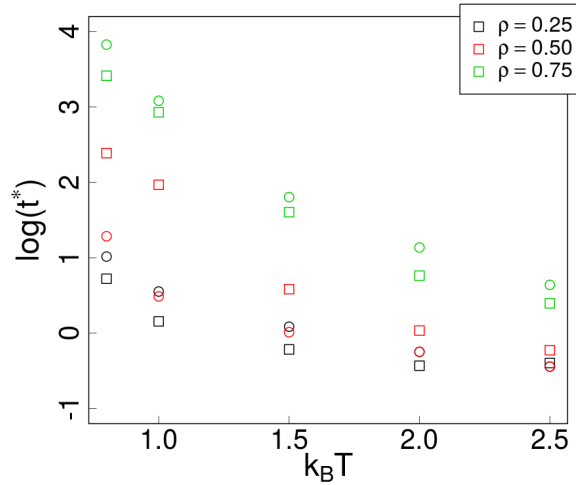

Figure 12: Correlation time for Langevin Dynamics simulations as function of $k_B T$ and density. The squares correspond to random, and the circles corresponds to co-aligned initial configuration.